

Supplementary Materials for

CDK13 cooperates with CDK12 to control global RNA polymerase II processivity

Zheng Fan, Jennifer R. Devlin, Simon J. Hogg, Maria A. Doyle, Paul F. Harrison, Izabela Todorovski, Leonie A. Cluse, Deborah A. Knight, Jarrod J. Sandow, Gareth Gregory, Andrew Fox, Traude H. Beilharz, Nicholas Kwiatkowski, Nichollas E. Scott, Ana Tufegdžić Vidaković, Gavin P. Kelly, Jesper Q. Svejstrup, Matthias Geyer, Nathanael S. Gray, Stephin J. Vervoort*, Ricky W. Johnstone*

*Corresponding author. Email: ricky.johnstone@petermac.org (R.W.J.); stephin.vervoort@petermac.org (S.J.V.)

Published 29 April 2020, *Sci. Adv.* **6**, eaaz5041 (2020)
DOI: 10.1126/sciadv.aaz5041

The PDF file includes:

Figs. S1 to S5

Other Supplementary Material for this manuscript includes the following:

(available at advances.sciencemag.org/cgi/content/full/6/18/eaaz5041/DC1)

Tables S1 to S5

Figure S1: CDK12 and CDK13 are functionally redundant for cancer cell survival (related to Figure 1).

A. Heat-map of Dependency Scores for 55 CDKs and cyclins in 496 non-hematological cancer cell lines from the Avana CRISPR public 19Q1 dataset. **B.** Box-plot comparisons of Dependency Scores for Cyclin K and CDKs 7, 9, 12 and 13 in 62 hematological versus 496 non-hematological cancer cell lines from the Avana CRISPR public 19Q1 dataset. **C.** Sanger sequencing chromatograms from MV4;11 WT and analog-sensitive (AS) clones spanning the gatekeeper residue coding region of CDK12 and CDK13 genomic loci. **D.** IGV screenshot of CDK12 and CDK13 loci for total RNA-seq analysis of MV4;11 WT and AS clones. **E.** Normalized read counts (\log_2 CPM) for CDK12, CDK13, cyclin K and Actin for total RNA-seq analysis of MV4;11 WT and AS clones. **F.** Western blot of MV4;11 WT and AS clones, representative of 3 independent experiments. **G.** Representative CTV vs PI dot-plots and proportion of PI-negative cells for each division of MV4;11 WT and AS clones treated with 1-NM-PP1 as indicated for 48 hours. PI incorporation assay of **H.** parental MV4;11 and **I.** parental THP1 cells treated with THZ531 as indicated for 48 hours. **J.** Representative CTV profiles, mean division number and cell division proportions of PI-negative parental MV4;11 cells treated with THZ531 as indicated for 48 hours. B represents 62 hematological and 496 non-hematological cell lines. G-J represent the mean \pm SEM of 3 independent experiments and student t-tests were performed for B and J (* $p < 0.05$, ** $p < 0.01$, *** $p < 0.001$).

Figure S2: Selective and dual CDK12 and CDK13 inhibition alters gene expression (related to Figure 2).

A. Log fold change gene expression volcano plots for MV4;11 WT clone treated with 10 μ M 1-NM-PP1 for 4 hours (relative to DMSO treatment). **B.** Gene ontology analysis of differentially expressed protein-coding genes for MV4;11 AS clones treated with 10 μ M 1-

NM-PP1 for 4 hours ($\text{Log}_2\text{FC} < -1$, Adj. p-value < 0.05 relative to DMSO treatment). **C.** qPCR analysis of *BRCA1* mRNA abundance (normalized to 5'ETS abundance) in MV4;11 WT and AS clones treated with 10 μM 1-NM-PP1 for 0.5, 1, 2, 4 and 6 hours. **D.** Gene set enrichment analysis (GSEA) plots for #1 CDK12^{AS/NULL}; CDK13^{AS/NULL} and #2 CDK12^{AS/NULL}; CDK13^{AS/AS} MV4;11 clones treated with 10 μM 1-NM-PP1 for 4 hours (ranked by Adj. p-value relative to DMSO treatment). **E.** Gene expression heatmap of the top 200 variably expressed genes in WT (non-edited) and CDK12 / CDK13 AS edited MV4;11 clones treated with DMSO (-) or 10 μM 1-NM-PP1 (+) for 4 hours and parental MV4;11 (PARENTAL) cells treated with DMSO (-) or 200nM THZ531 (+) for 6 hours. Difference from row mean for the top 200 variably expressed genes is presented. C is representative of the mean \pm SEM of four biologically independent replicates and Dunnett's multiple comparison test were performed (* Adj.p < 0.05 , ** Adj.p < 0.01 , *** Adj.P < 0.001 , **** Adj.P < 0.0001).

Figure S3: Dual CDK12 and CDK13 inhibition causes alternative polyadenylation (related to Figure 2).

A. MISO analysis of total RNA-seq data for parental MV4;11 cells treated with THZ531 for 6 hours (100nM – top; 200nM – bottom). Column A of table represents legend for doughnut plots. Data is representative of 3 biologically independent experiments. **B.** Representative IGV profile of total RNA-seq and 3'RNA-seq analysis of alternative last exon usage for parental MV4;11 cells treated with THZ531 as indicated for 6 hours. Scale bars represent 50kb **C.** qPCR analysis of *ASCC3* long and short isoform mRNA abundance (normalized to 5'ETS abundance) in parental MV4;11 cells treated with THZ531 as indicated for 6 hours. **D.** MA plots representing proximal and distal 3' UTR peak shifts for WT MV4;11 clone treated with 10 μM 1-NM-PP1 for 4 hours. **E.** MA plots and **F.** quantitation of genes with a

significant change in proximal or distal 3'UTR peak signal in parental MV4;11 cells treated with 200nM THZ531 for 6 hours (relative to DMSO treatment). **G.** Representative IGV profiles of differential 3'UTR peak usage for MV4;11 AS clones treated with 10 μ M 1-NM-PP1 for 4 hours. Scale bars represent 10kb. C represents the mean \pm SEM of three biologically independent replicates and student t-test was performed (** $p < 0.01$, *** $p < 0.001$).

Figure S4: CDK12 and CDK13 cooperate to control POLII processivity by modulating the phosphorylation of POLII CTD (related to Figure 3).

A. Quantitation of Log₂ fold change (THZ531 or NMPP1 relative to DMSO) of POLII CTD phosphor- western blots for Figure 3E). POLII CTD phospho-signal was normalized to ACTIN. **B.** Average gene profiles of 9552 expressed genes for total and phospho-serine 2 POLII ChIP-seq analysis of MV4;11 WT cells treated with 10 μ M 1-NM-PP1 for 4 hours. **C.** Transcription start site (TSS) and end site (TES) average profiles of 9552 expressed genes for total POLII ChIP-seq analysis of AS MV4;11 clones treated with 10 μ M 1-NM-PP1 for 4 hours. **D.** POLII processivity index is calculated as the fold change ratio of total POLII ChIP reads or PRO-seq reads mapping to the 5' region (TSS + 1000bp) over the 3' region (TES – 1000bp) of the gene body. **E.** POLII processivity index for total POLII ChIP subset by gene length quartiles in WT and AS MV4;11 clones treated with 10 μ M 1-NM-PP1 for 4 hours. **F.** Average gene profiles of 9552 expressed genes for total and phospho-serine 2 POLII ChIP-seq analysis in parental MV4;11 cells treated with THZ531 as indicated for 6 hours. **G.** POLII processivity index for parental MV4;11 cells treated with THZ531 as indicated for 6 hours. **H.** TSS and TES average profiles of 9552 expressed genes for total Pol II ChIP-seq analysis of parental MV4;11 treated with THZ531 as indicated for 6 hours. **I.** Average gene profiles and processivity index of 9552 expressed genes for PRO-seq analysis of parental

MV4;11 cells treated with THZ531 as indicated for 6 hours. **J.** TSS and TES average profiles of 9552 expressed genes for PRO-seq analysis of parental MV4;11 treated with THZ531 as indicated for 6 hours. A represents the mean \pm SEM of 3 biologically independent replicates. E represents 9552 expressed genes subset by gene length quartile. G and I represent 9552 expressed genes. Student t-tests were performed for A, G and I (** $p < 0.01$, **** $p < 0.0001$).

Figure S5: Dual inhibition of CDK12 and CDK13 perturbs POLII elongation by altering POLII processivity and elongation rate (related to Figure 4).

A. Schematic overview and **B.** representative IGV images for DRB release PRO-seq assay of parental MV4;11 cells treated with 100nM or 200nM THZ531 as indicated. Scale bars represent 50kb. **C.** Average gene profiles for DRB release PRO-seq analysis of 368 genes in WT and #2 CDK12^{AS/NULL}; CDK13^{AS/AS} MV4;11 clones treated with 10 μ M 1-NM-PP1 as indicated in 4A. **D.** Average gene profiles for DRB release PRO-seq analysis of 368 genes in parental MV4;11 cells treated as indicated in S4C. Heat map analysis of **E.** PRO-seq signal and **F.** Log₂ fold change PRO-seq signal (DMSO relative to THZ531) in parental MV4;11 cells treated with THZ531 as indicated post-washout of DRB. **G.** Pol II elongation rate and **H.** Log₂ fold change in Pol II elongation rate (relative to DMSO) in #2 CDK12^{AS/NULL}; CDK13^{AS/AS} MV4;11 clone treated with 10 μ M 1-NM-PP1 for 25 minutes post DRB wash-out. **I.** Pol II elongation rate and **J.** Log₂FoldChange in Pol II elongation rate (relative to DMSO) in parental MV4;11 cells treated as indicated with THZ531 at 25 minutes post DRB wash-out. **K.** Venn diagram representing number of genes exhibiting a significant change in 3'UTR peak signal (proximal or distal) for i) Flp-In HEK293 cells expressing R749H- and H1108Y mutant Rpb1 following induction with doxycycline and treatment with α -amanitin (compared to Flp-In HEK293 cells expressing wildtype Rpb1) and; ii) HEK293T cells treated

with 400nM THZ531 for 6 hours (Adj. P-value <0.05). **L.** Proportion of genes with a significant change in proximal or distal 3'UTR peak signal for Flp-In HEK293 cells expressing R749H and H1108Y mutant Rpb1 (compared to Flp-In HEK293 cells expressing wildtype Rpb1) and HEK293T cells treated with 400nM THZ531 for 6 hours. **M.** Schematic overview of POLII elongation rate and pausing defect. G, H, I and J are representative of 368 genes and student t-test was performed for G and I (***) p<0.001).

FIGURE S1

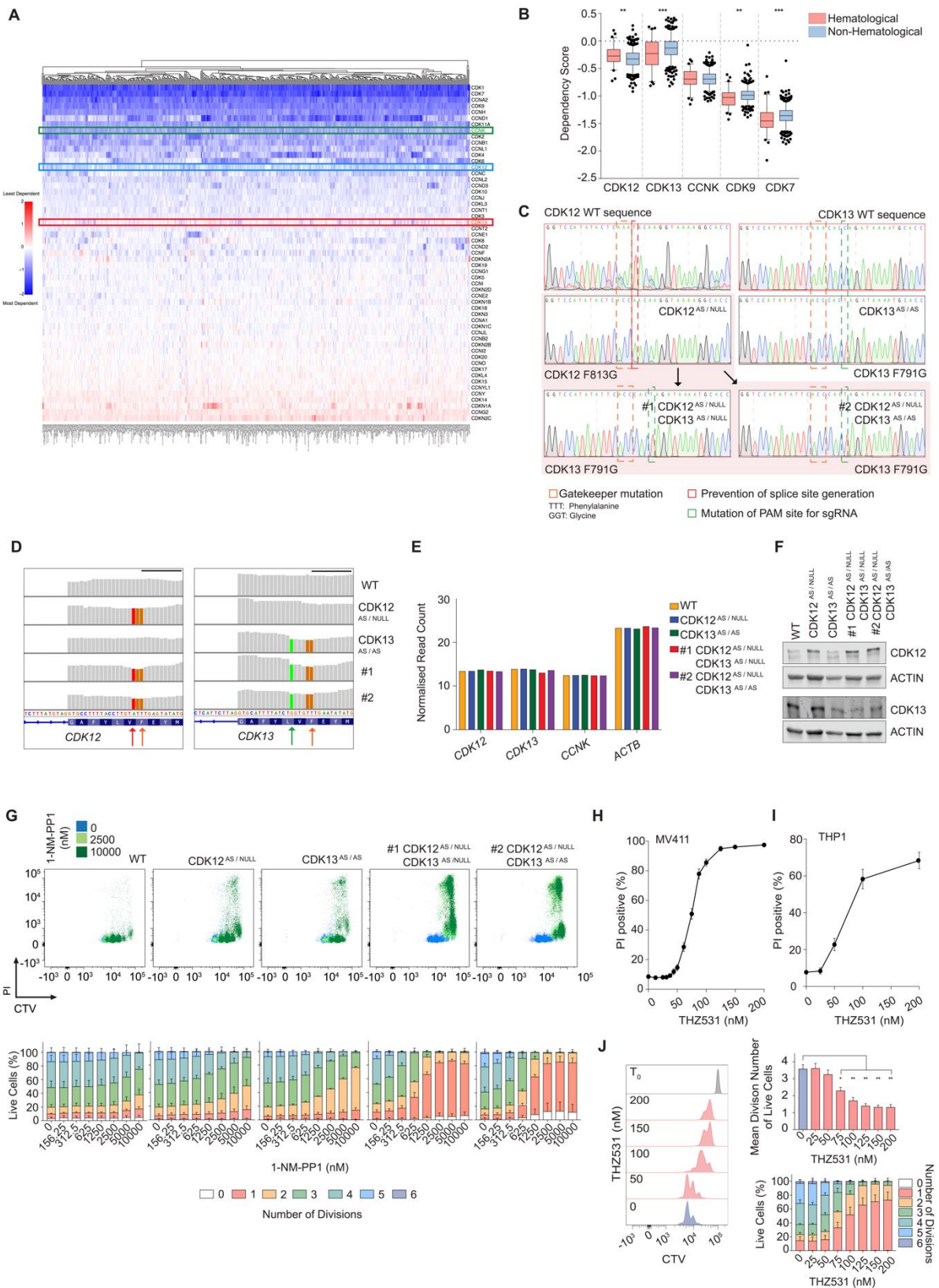


FIGURE S2

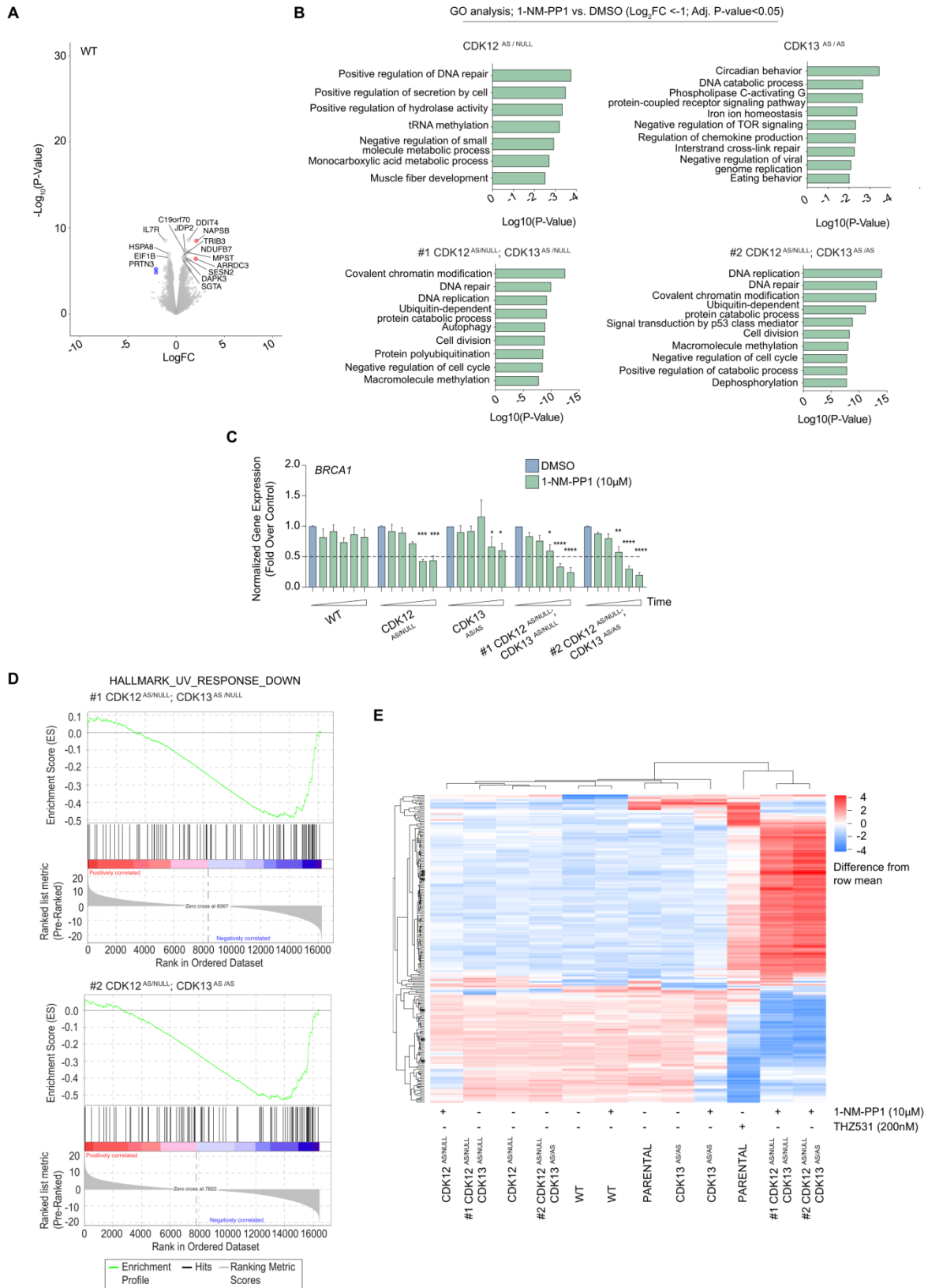


FIGURE S3

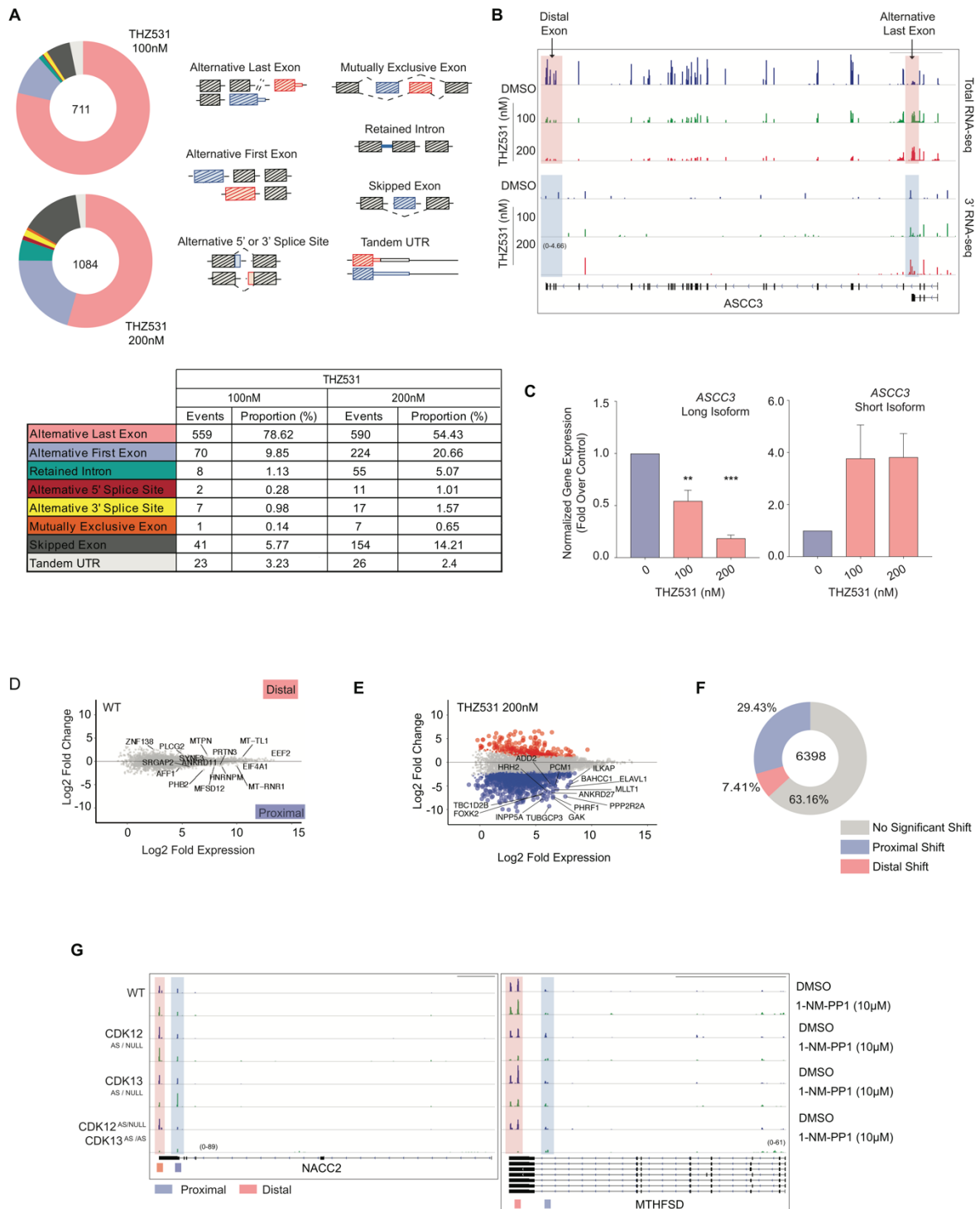


FIGURE S4

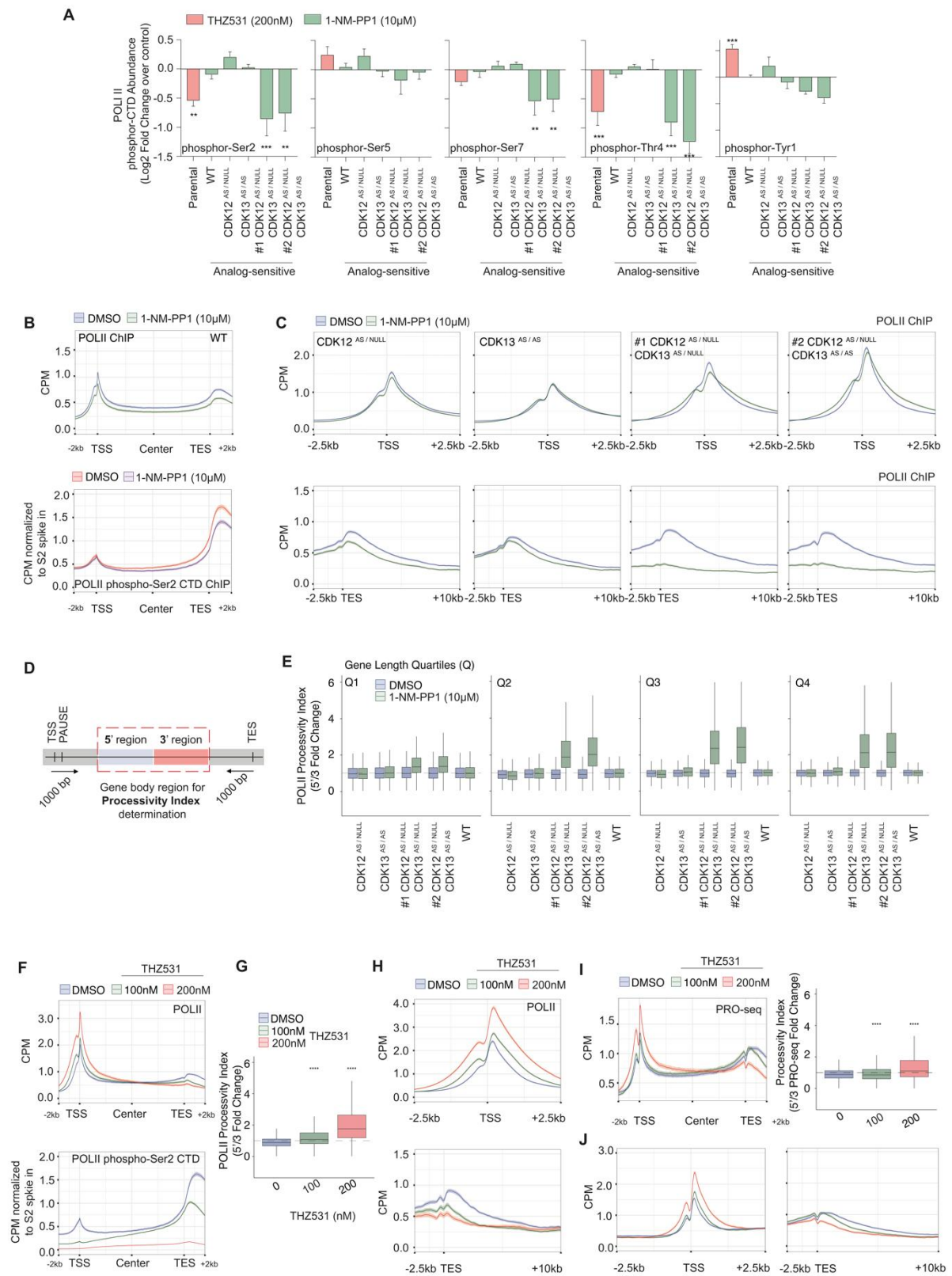


FIGURE S5

